JACS
JOURNAL OF THE AMERICAN CHEMICAL SOCIETY
pubs.acs.org/JACS
Article

Kinetically Programmed Signaling Cascades for Molecular Detection

Guichi Zhu, Dominic Lauzon, Carl Prévost-Tremblay, Arnaud Desrosiers, Bal-Ram Adhikari, and Alexis Vallée-Bélisle*

Cite This: J. Am. Chem. Soc. 2025, 147, 39452−39463
Read Online

ABSTRACT: Upon external stimulation, living cells activate a series of precisely programmed signaling cascade reactions that efficiently convert multiple stimuli into relevant output signals, thereby maintaining physiological homeostasis. These naturally evolved molecular networks have recently inspired the development of new chemical strategies in fields ranging from synthetic biology to molecular computing, drug delivery, and biosensing systems. While some studies have begun to explore how programming the thermodynamics of these bioinspired chemical systems can optimize their performance, the impact of programming their kinetics remains largely unexplored. Here, we leveraged the modularity and programmability of DNA chemistry to develop a simple DNA-based signaling cascade to measure the concentration of specific molecules and investigated how programming its kinetics affects its performance. This signaling cascade comprises four modules (input, receptor, processor, and output) and three molecular interactions for which we have characterized all intrinsic rate constants. Through simulations and experiments, we demonstrated that careful kinetic programming can significantly enhance the rate, gain, and sensitivity of the signaling cascade output. We further illustrated the versatility and modularity of this cascade by adapting it for the detection of four different molecules (small molecules and proteins). We also showed that it can be readily adapted into a rapid, one-step, inexpensive electrochemical sensor enabling therapeutic drug monitoring (TDM) at home directly from a drop of blood. We believe that similar kinetically programmed signaling cascades could be developed for a wide range of chemical applications, allowing complex, multistep workflows to be streamlined into rapid, single-step reactions.

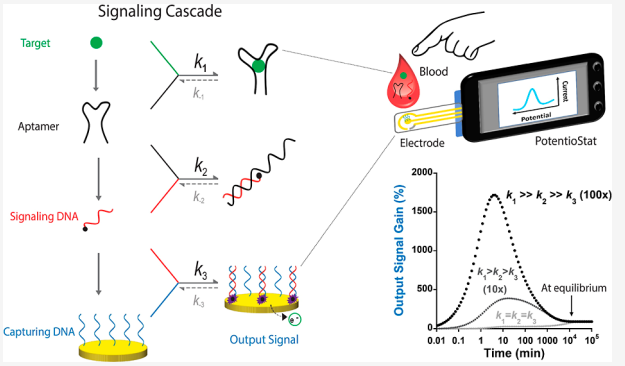

INTRODUCTION

Biochemical mechanisms have inspired numerous key developments in chemistry. From the concepts of molecular recognition,[1] self-assembly,[2,3] and molecular libraries[4,5] to the development of greener and more efficient enzyme-inspired catalysts,[6−8] nature has provided multiple sources of inspiration to drive innovation in chemistry. More recently, the recreation and mathematical validation of various specific biochemical mechanisms, including molecular switches,[9] allostery/cooperativity,[10−12] multivalent interaction,[13,14] and molecular self-assembly,[15,16] have significantly contributed to develop a new generation of programmable molecular machines with various applications in smart materials, molecular transporters, sensing, and logic gates.[17,18]

Signaling cascades represent another key biochemical mechanism[19] that has started to attract the attention of chemists. These finely tuned molecular network reactions, which typically display modular and hierarchical architectures including input, receptor, processor, and output modules (Figure 1a),[20,21] have evolved to detect a wide array of chemical inputs to control and optimize cell activity, division, and differentiation.[22] Inspired by these natural intracellular signaling cascades, researchers have recently started to develop artificial molecular networks for applications in synthetic biology,[23] molecular computing,[24] and drug delivery.[25,26] Biochemists, for example, have first started to modify and reprogram natural signaling cascades.[20,21] Building on the high programmability of DNA chemistry, chemists have also begun to design simplified synthetic cascades for diverse applications. For instance, Winfree's group has developed DNA-based molecular computers that can resolve mathematical problems.[27,28] Tan and colleagues have engineered artificial signaling systems to study cellular adaptability, membrane functions, and immune responses.[29−31] Meanwhile, Willner's lab has introduced constitutional dynamic chemistry (CDC)-based networks[32] for applications in intracellular imaging and gene therapy.[33] While several of these bioinspired proof-of-concept systems have started to investigate how programming thermodynamic parameters affects performance, the role of

Received: July 15, 2025
Revised: September 3, 2025
Accepted: September 5, 2025
Published: October 16, 2025

https://doi.org/10.1021/jacs.5c12059
J. Am. Chem. Soc. 2025, 147, 39452−39463

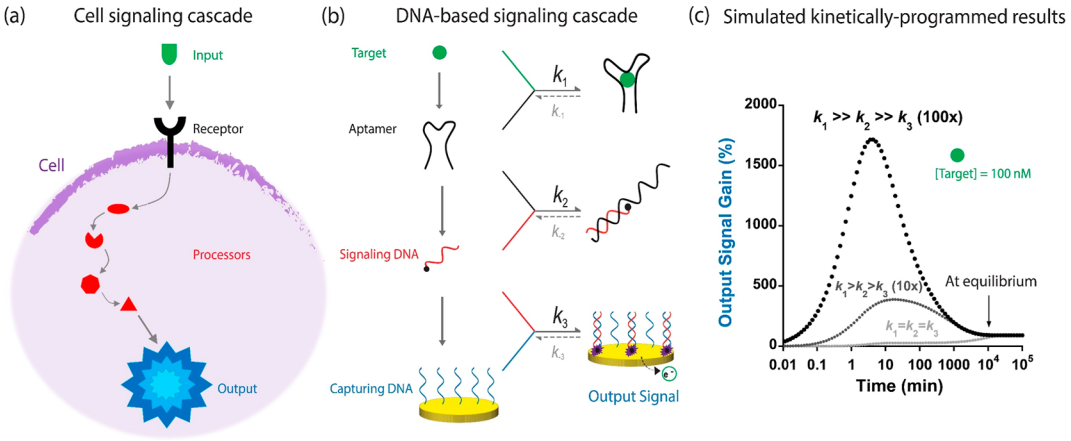

Figure 1. Kinetically programmed signaling cascades for molecular detection. Inspired by cell signaling cascades (a), we have created a similar 4 components DNA-based signaling cascade that transduces the binding of a specific target molecule into a convenient electrochemical output (b). In the presence of a target molecule (input), a DNA aptamer (receptor) is sequestered and unable to hybridize with its complementary redox-labeled signaling DNA (processor). This latter can then bind to the capturing DNA (output) on the electrode surface and generate high electrochemical signal. In the absence of the target molecule, the DNA aptamer remains unbound and available to hybridize with its complementary signaling DNA, inhibiting the formation of the signaling-capturing DNA duplex on the surface of the electrode, thus generating low electrochemical currents. (c) Simulation of this proposed signaling cascade reveals that its output signal gain and response time can be drastically enhanced by programming the kinetics of the three reactions such that $k_1 \gg k_2 \gg k_3$ (100x). The output signal gain (%) represents the percentage of signaling-capturing DNA duplex variation (variation in current) when adding 100 nM of target (see Figure S1 for complete simulation parameters).

programming the kinetics of their components remains largely unexplored. Recently, various strategies have been developed to regulate the kinetics of DNA interaction, including modifying DNA sequences and compositions,[34] adjusting hybridization conditions (such as pH, temperature, salt concentration, and organic solvents),[35] utilizing multivalent or allosteric mechanisms,[14] and employing toehold-mediated strand displacement reactions.[36−39] However, these approaches generally focus on controlling individual hybridization events and rarely address how kinetic programming can influence sequential, multistep systems like signaling cascades.

One chemistry field that stands to benefit significantly from signaling cascades is biosensing. Gold-standard chemical assays for molecular diagnostic applications such as enzyme-linked immunosorbent assay[40] and polymerase chain reaction[41] typically involve multistep protocols that are intensive in reagents and washes, and frequently depend on precise thermal regulation and complex optical detection platforms. Simpler to use point-of-care sensors, such as lateral flow assays, offer faster workflows (10−15 min), but these still require multiple steps (5−6 steps) and typically provide only qualitative results (i.e., yes/no answers). In this study, we developed a simple DNA-based signaling cascade containing four modules and three molecular interactions, designed to detect molecular inputs through a convenient electrochemical output (Figure 1b). In addition to demonstrating the modularity, potential universality, and usefulness of this cascade, we showed that programming its kinetics significantly enhances its rate, gain, and sensitivity (Figure 1c). We also discussed the advantages of this signaling cascade mechanism over existing sensing strategies and explored its broader potential for various chemical applications.

RESULTS

A DNA-Based Signaling Cascade for Molecular Detection. We designed our DNA-based signaling cascade by drawing inspiration from the modularity and hierarchical arrangement found in intracellular signaling cascades, which are typically composed of input, receptor, processor, and output modules.[20,21] Although this signaling cascade could, in principle, be built using proteins, we selected DNA chemistry as our building module for several reasons. First, DNA sequences can be specifically chosen to bind a wide range of molecular targets (e.g., aptamers).[42,43] Second, these DNA aptamers can be readily engineered into molecular switches[44] or can be allosterically controlled by simply binding to their complementary DNA sequences.[45] Third, we have previously shown that DNA hybridization of redox-labeled DNA on a gold surface provides an efficient, quantitative electrochemical signal output for blood analysis with limited or no biofouling.[46−48] Fourth, the selectivity of DNA−DNA interactions enables multiple DNA reactions to proceed simultaneously in the same sample, enabling the multiplexed detection of various analytes.[49−51] Finally, DNA hybridization is readily tunable in both thermodynamic and kinetic dimensions.[37,52−55] Our proposed signaling cascade is composed of four modules and three molecular interactions (Figure 1b). The "input" module (i.e., target molecule) can be specifically recognized by the "receptor" module made of an unmodified DNA aptamer (see interaction k_1). The "processor" module is composed of redox-labeled signaling DNA, which operates through an allosteric inhibition mechanism, whereby the DNA aptamer binds and inhibits the signaling DNA when the aptamer remains unbound (see interaction k_2). This allosteric mechanism is based on previous work demonstrating that target binding to an aptamer typically prevents or inhibits its hybridization to its complementary sequence.[56] Finally, the "output" module consists of the signaling DNA hybridizing to its complementary DNA sequence, called capturing DNA, attached to a gold electrode, which generates an electrochemical signal upon binding (see interaction k_3).[46]

Kinetics Programming of the Signaling Cascade Enhances Its Performance. We first explored the kinetics of our signaling cascades through numerical simulations by employing rate constants typical of DNA−DNA interactions.[57]

https://doi.org/10.1021/jacs.5c12059
J. Am. Chem. Soc. 2025, 147, 39452−39463

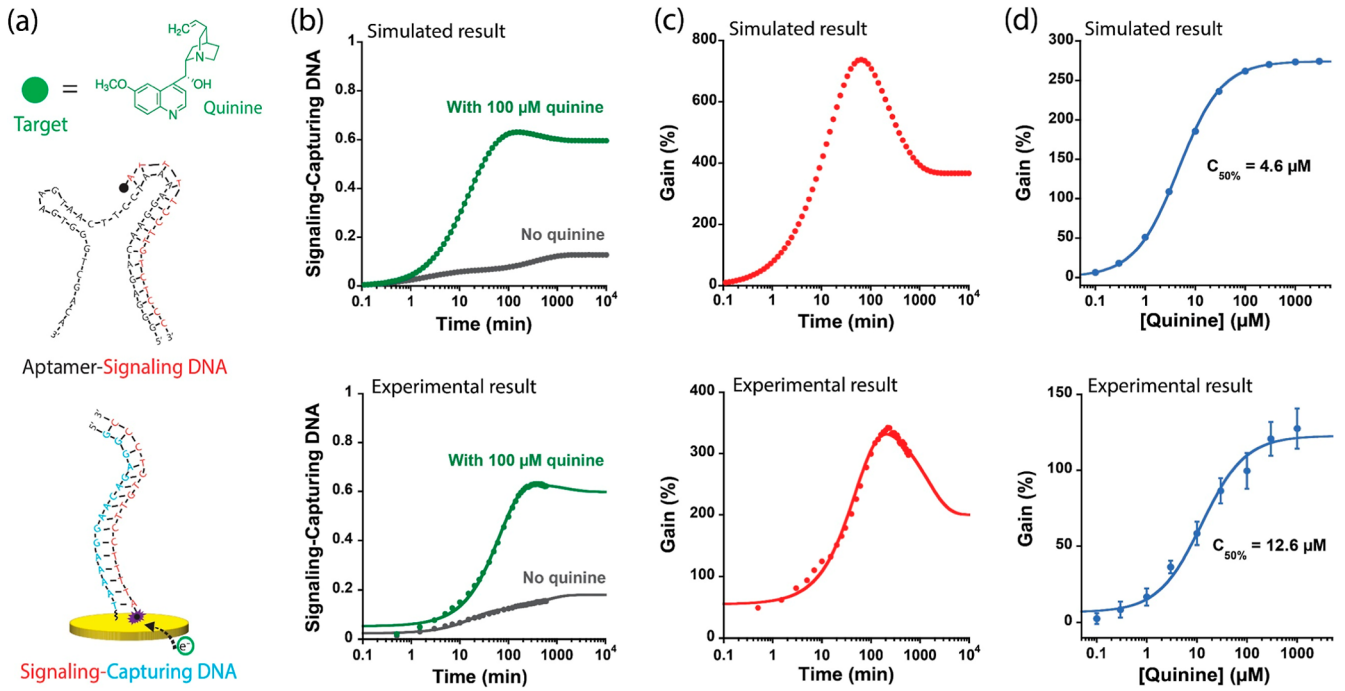

Figure 2. (a) A kinetically programmed DNA-based signaling cascade engineered for quinine detection. Simulated and experimental kinetics (b), gain (c), and dose–response curves (d) of the kinetically programmed assay for the detection of quinine (5 min). The gain represents the percentage of signaling-capturing DNA duplex change between the sample containing or not containing quinine $(((S_{withquinine} - S_{noquinine})/S_{noquinine}) \times 100\%)$. $C_{50\%}$ represents the target concentration at which the observed signal gain is half its maximal value. The simulations were performed using 100 μM quinine, 100 nM aptamer, 100 nM signaling DNA, and 100 nM capturing DNA. The experiments were performed in 1 mL of phosphate-buffered saline solution containing 100 μM quinine, 100 nM aptamer, and 100 nM signaling DNA, while maximum density of capturing DNA was obtained by functionalizing our electrodes using 300 nM of capturing DNA (see electrode fabrication and electrochemical measurement section in Supporting Information). Of note, the experimental signaling cascade shows a typical one-site binding with "81-fold" dynamic range from 1.4 μM to 113 μM.[17,65] The error bars show the standard deviation obtained from three sensors.

When the affinity of all interactions and their rate constants, k_1, k_2, and k_3, are set equal (for example, $k_1 = k_2 = k_3 = 0.01$ nM^{-1} min^{-1}), we found that the signaling cascade only produces a 91% output signal gain at equilibrium (Figure 1c, light gray curve). Since aptamer typically binds non-nucleic acid targets faster than DNA–DNA interactions form ($k_1 > k_2$) and since DNA hybridizes more rapidly in solution than on surfaces ($k_2 > k_3$), we further explored the kinetics of the signaling cascade using $k_1 > k_2 > k_3$. When $k_1 = 10k_2 = 100k_3$, the signaling cascade produced a much higher output signal gain (387%) before reaching equilibrium (Figure 1c, dark gray curve). When employing an even more significant kinetic difference, for example, $k_1 = 100k_2 = 10{,}000k_3$, the output signal gain was further enhanced to 1716% before reaching equilibrium (Figure 1c, black curve). The larger gain obtained via such kinetics programming is mainly attributed to the lower signal background produced in the absence of a target, since the unbound aptamer can rapidly bind and inactivate the signaling DNA (k_2) before it has time to reach the sensor surface (k_3) (Figure S1). Overall, these simulations proved that kinetically controlled signaling cascades are promising and that their performance can even be further optimized through kinetics programming.

Engineering a Signaling Cascade for the Detection of Quinine. As an initial proof-of-principle to validate our kinetically programmed signaling cascade, we selected quinine, a popular antimalarial drug,[58] as the target molecule in our assay (Figure 2a). Although quinine is among the most widely used antimalarial drugs, it is associated with several dose-dependent toxicities, such as cinchonism, hypoglycemia, and hypotension.[59] Consequently, home-based strategies for monitoring therapeutic agents, including quinine and other medications, could substantially enhance treatment efficacy and safety.[60] To develop a signaling cascade to detect quinine, we employed a well-characterized quinine-binding aptamer[61,62] and designed a 16-nucleotides redox-labeled signaling DNA complementary to both the quinine-binding aptamer and a capturing DNA (16-nucleotides) attached to a gold surface (Figure 2a). We then employed electrochemistry (Figure 1b, k_3) to quantify the concentration of the single-stranded redox-labeled signaling DNA via its hybridization to its electrode-bound complementary DNA sequence (capturing DNA). This specific electrochemical signaling mechanism (k_3), previously developed and characterized by us and others,[46,63,64] demonstrates great robustness and low interference when deployed in complex samples such as whole blood. Briefly, the 16-nucleotides signaling DNA possesses a redox-active methylene blue attached to its 5′-extremity, which is brought next to the electrode surface upon hybridization to its surface-bound complementary DNA (capturing DNA). Upon approaching the gold electrode surface, the methylene blue undergoes electron transfer, thereby generating an electrochemical signal that correlates with the concentration of hybridized signaling DNA. We designed this 16-nucleotide signaling DNA so that it can also hybridize to the 5′-extremity of the aptamer sequence, but other binding locations could have also been explored and tested. We hypothesized that quinine binding will stabilize the folded conformation of the

https://doi.org/10.1021/jacs.5c12059
J. Am. Chem. Soc. 2025, 147, 39452–39463

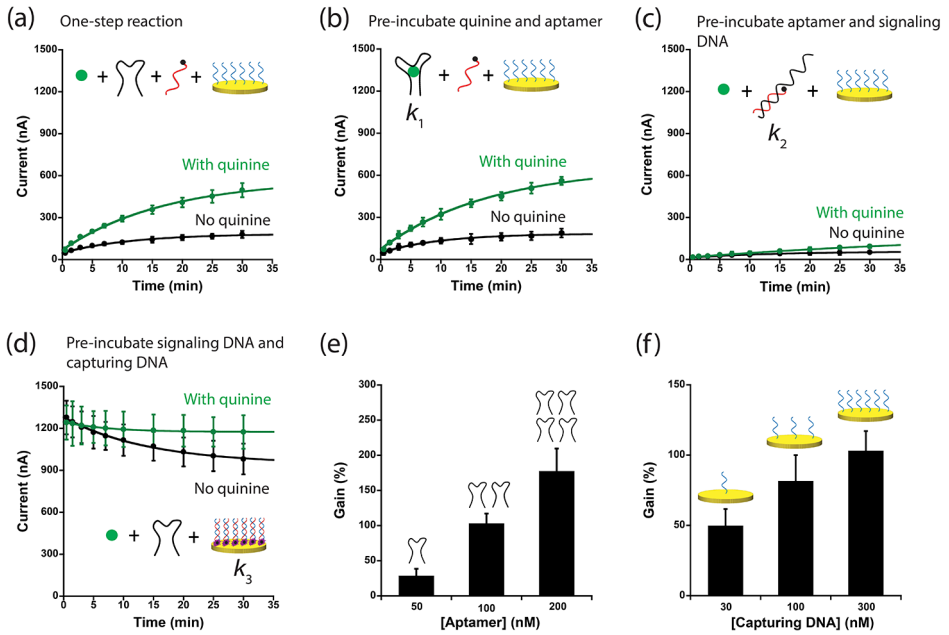

Figure 3. Quinine detection cascade is kinetically controlled and may be further optimized by tuning the reaction rates ($k_1 > k_2 > k_3$). Quinine assays were conducted under the following conditions: (a) a one-step reaction; (b) preincubation of quinine with its aptamer for 30 min; (c) preincubation of the aptamer with signaling DNA for 30 min; and (d) preincubation of the signaling and capturing DNA for 30 min. (e) Increasing k_2 relative to k_3 by raising the aptamer concentration improved the gain. The gain was obtained after 5 min of reaction. (f) Reducing k_3 relative to k_2 by increasing the density of capturing DNA on the electrode surface also improved the gain. The gain was obtained after 5 min of reaction. The error bars show the standard deviation obtained from three sensors.

aptamer and therefore inhibit its association with its complementary signaling DNA sequence.

We first modeled the expected cascade response by employing the experimentally determined kinetic parameters (association rate constant, k_{on} and dissociation rate constant, k_{off}) of all three reactions involved in the cascade: quinine-aptamer binding (Figure S2a), aptamer-signaling DNA hybridization (Figure S2b), and signaling DNA-capturing DNA hybridization (Figure S2c). We found that the rate of complex formation between quinine and its aptamer, k_1, is 258 times faster (Figure S2d) than the rate of aptamer-signaling DNA hybridization in solution, k_2 (negative charges on DNA typically slow DNA hybridization rates). We also found that the hybridization rate of the signaling DNA on the surface-bound capturing DNA, k_3, is 42 times slower than that of k_2 (Figure S2d). This ensures that most signaling DNAs will be rapidly bound and inhibited by the aptamer in the absence of the target before reaching and hybridizing the complementary capturing DNA on the surface. We performed the first simulations and experiments using a high concentration of quinine (100 μM) (Figure 2b,c) to ensure maximal binding and sequestration of the aptamer (the K_D of quinine-aptamer is 0.87 μM, see Figure S2). We selected a 100 nM aptamer concentration to enable detection limit in the low nM range of the target in the case where the aptamer would display strong affinity for its target (e.g., K_D < 10 nM). The aptamer concentration was also set equal to the signaling DNA concentration to enable complete inhibition of this later in the absence of target (100 nM of aptamer hybridizes to 100 nM of signaling DNA). Of note, 100 nM of signaling DNA was also shown to provide sufficient electrochemical current for reaction times below 10 min.[46] In the absence of quinine, most signaling DNA rapidly hybridizes the aptamer, and only a small fraction remains available to hybridize with the capturing DNA (see the gray curve, Figure 2b, top). A second slower transition represents the slow equilibration process between the kinetically trapped signaling DNA in the rapidly formed aptamer-signaling DNA complex and the signaling-capturing DNA complex (Figure S3a). In the presence of quinine, the aptamer is rapidly sequestered (or inhibited), and the signaling DNA preferentially hybridizes to the capturing DNA (see the green curve, Figure 2b, top). A second slower phase, leading to a reduction in the electrochemical signal, represents the slow equilibration between the kinetically trapped signaling DNA in the signaling-capturing DNA complex and its dissociation and subsequent association with the free aptamer (Figure S3b).

We then tested these simulations by deploying the signaling cascade in a phosphate-buffered saline solution and found that all predicted transitions were also detected in the experiment (Figure 2b, bottom). As noticed in our initial simulations (Figure 1c), the maximal gain in the presence of quinine also takes place well before equilibrium is reached (Figure 2c). Of note, the smaller maximal gain obtained experimentally (342% versus 738% for simulation) may be attributable to the fact that the simulation does not consider that the capturing DNA is attached to the surface. This may lead to a decrease in k_{on} with time as the surface becomes more crowded with negatively charged DNA. We also noted that the simulation and experimental data revealed similar dose−response curves and $C_{50\%}$ after a reaction time of 5 min (4.6 μM versus 12.6 μM, respectively; see Figure 2d). We noted that this dose−response curve is approximately shifted by 10-fold to higher concentrations of targets compared to the original aptamer K_D (0.87 μM, see Figure S2). Simulations further revealed that longer reaction times increased the $C_{50\%}$ values, resulting in reduced sensitivity (Figure S4). For instance, $C_{50\%}$ increased from 1.9 to 33.9 μM for reaction times between 1 min and equilibrium, respectively (Figure S4e). This can be attributed

https://doi.org/10.1021/jacs.5c12059
J. Am. Chem. Soc. 2025, 147, 39452−39463

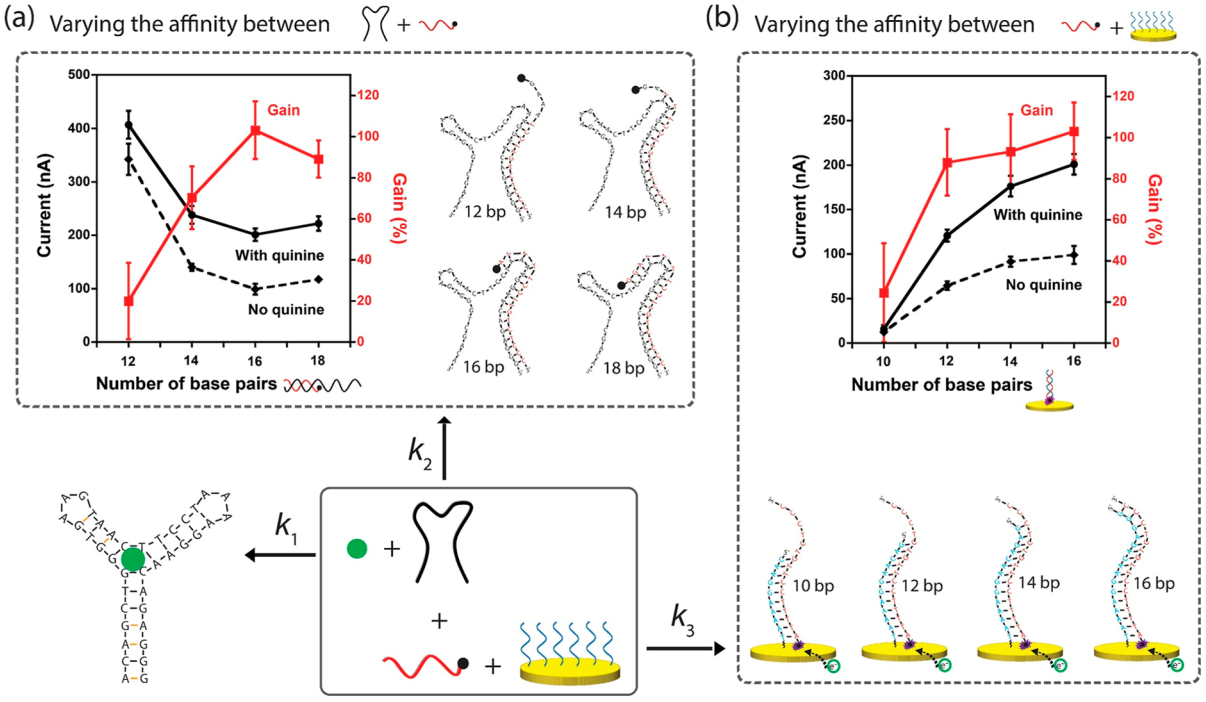

Figure 4. Kinetically programmed DNA-based signaling cascade is relatively insensitive to variations in affinities between its interacting components. (a) Increasing the affinity between the aptamer and signaling DNA (K_{D2}) (from 14 to 18 Watson−Crick base pairs; 5.5 kcal/mol variation) did not significantly affect the gain of the cascade (between 70 and 103% after 5 min of reaction in the presence of 100 μM quinine). (b) Increasing the affinity between the signaling DNA and capturing DNA (K_{D3}) (12 to 16 Watson−Crick base pairs; 6.0 kcal/mol variation) produced only a slight gain change from 88 to 103% after 5 min of reaction in the presence of 100 μM quinine. The error bars show the standard deviation obtained from three sensors.

to the presence of the signaling DNA that competes with the target for aptamer binding.[56] As a result, although a larger gain is observed at around 60 min when detecting high quinine concentrations (100 μM, Figure 2c, top), comparable gains are achieved at 5 and 60 min reaction times when detecting concentrations near the detection limit (e.g., 1 μM; see Figure S4f). Considering that most sensing applications (particularly point-of-care diagnostics) benefit from rapid response times (ideally under 10 min) and low detection limits, we selected a reaction time of 5 min for all subsequent experiments. Of note, the dynamic range of the signaling cascade exhibits the typical 81-fold range, consistent with that of a one-site binding system, with optimal sensitivity ranging from $C_{50\%}/9$ (10% signal) to $C_{50\%} \times 9$ (90% signal).[17,65] Overall, the strong agreement between the simulation and the experiments suggests that our signaling cascade works according to our proposed model.

The Signaling Cascade Is Kinetically Controlled. As shown in the simulation results (Figures 1c and S1), the performance of the signaling cascade is expected to be strongly dependent on the kinetics of its component. To validate this experimentally, we artificially mimicked an increase in the different reaction rates (Figure 3). For example, quinine was premixed with its aptamer before introducing the signaling and capturing DNA to artificially increase k_1 relative to k_2 and k_3. Given that k_1 is already considerably faster than k_2 and k_3 (see Figure S2d), no significant kinetic variation was observed between the one-step reaction (Figure 3a) and the quinine-aptamer preincubation (Figure 3b). Simulations also indicate that if k_1 remains equal to or faster than k_2, similar sensing performances will be achieved (Figure S5). In contrast, a marked decrease in sensing performance was noted when the aptamer and signaling DNA were preincubated for 30 min prior to the addition of quinine and capturing DNA, effectively simulating a scenario in which k_2 exceeds both k_1 and k_3 (Figure 3c). This observation indicates that after the aptamer-signaling DNA complex is established, the strong binding affinity and slow dissociation of the duplex hinder the signaling DNA from binding the capturing DNA within the duration of the experiment ($t_{1/2}$ of aptamer-signaling DNA duplex is ~630 min, see Figure S2b). Finally, preincubation of the signaling and capturing DNA for 30 min prior to addition of quinine and the aptamer resulted in a very high signal background, reflecting a kinetic condition where k_3 exceeds both k_1 and k_2 (Figure 3d). Without quinine, the initially high background current declines slowly over time as signaling DNA detaches from the capturing DNA and associates with the aptamer ($t_{1/2}$ of the signaling-capturing DNA duplex is ~592 min, see Figure S2c). In contrast, when quinine is present, the signal remains largely unchanged because the aptamer preferentially binds quinine, preventing it from sequestering any dissociated signaling DNA. Overall, these findings show that our one-step, kinetically programmed signaling cascade achieves higher gain when the reaction rates are programmed such that $k_1 > k_2 > k_3$.

To further improve the gain and performance of our signaling cascade, we explored how the assay can be further optimized by programming k_1, k_2, or k_3 via various strategies. Previous simulations showed that enlarging the rate differences among k_1, k_2, and k_3 enhances the gain by reducing the background and increasing the signal (Figure S1). Since the difference in reaction rate between k_2 and k_3 in our assay could be further increased (~42 times, see Figure S2d), we first selectively increased k_2 over k_3 by raising the concentration of the aptamer from 50 to 200 nM (Figure S6a). This increased

https://doi.org/10.1021/jacs.5c12059
J. Am. Chem. Soc. 2025, 147, 39452−39463

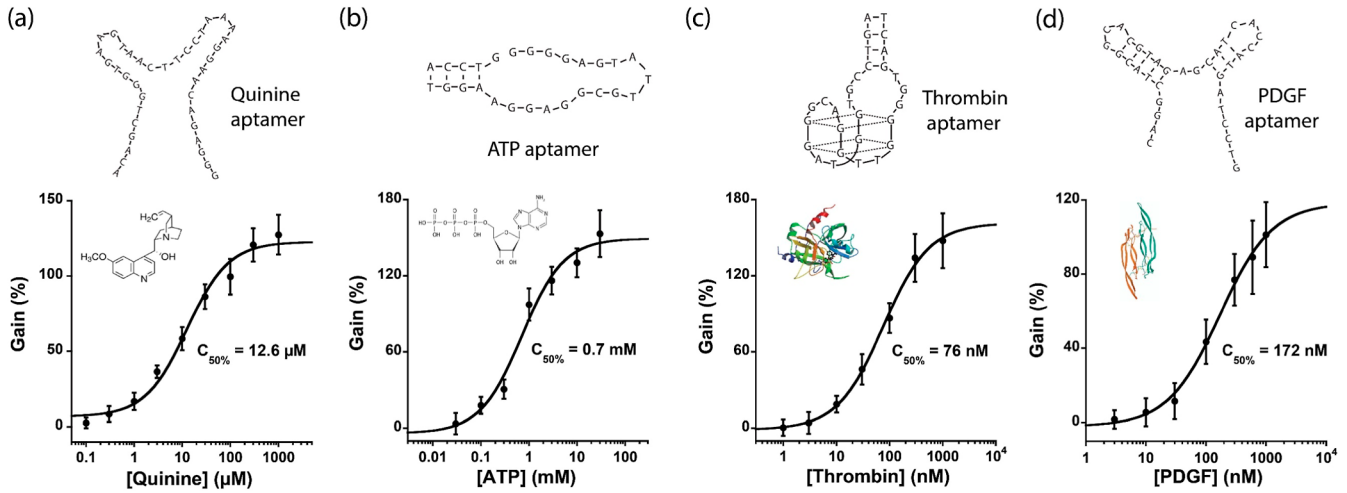

Figure 5. Kinetically programmed DNA-based signaling cascade can be easily adapted to create a variety of "signal-on" sensors with minimal optimization. Here, we employed 16-nucleotide signaling DNA to develop (a) a quinine sensor, (b) an ATP sensor, (c) a thrombin sensor, and (d) a PDGF sensor. The gain was measured by comparing the electrochemical current with or without the target following a 5 min reaction time. The detection limits of each sensor were found to be proportional to the K_D of the aptamers: 2.2 μM (quinine sensor), 0.15 mM (ATP sensor), 17 nM (thrombin sensor), and 50 nM (PDGF sensor) (see Figure S9). All binding curves displayed the classic hyperbolic 81-fold dynamic range expected for one-site binding system.[17,65] The error bars show the standard deviation obtained from three sensors.

k_2 (and thus the difference between k_2 and k_3) by approximately 2.4 times (Figure S6b), improving the gain from ∼28 to ∼177% (Figure 3e). Of note, increasing the concentration of aptamer increases the gain by diminishing the signal background (Figure S7). However, employing an aptamer/signaling DNA ratio higher than two also shifts the binding curve to higher concentrations of targets. This effect, however, remains much smaller in the case of the kinetic assay (i.e., when not performed until equilibrium; see Figure S7). This also provides a simple strategy to tune the dynamic range of this sensor.

In a second attempt to increase the difference between k_2 and k_3, we also decreased the density of the capturing DNA at the electrode surface, which is an approach to accelerate signaling-capturing DNA hybridization kinetics by lowering the local charge density and reducing electrostatic repulsion near the electrode surface (DNA is charged negatively).[66] In order to reduce capturing DNA surface density, we employed lower DNA concentrations (300 nM, 100 nM, and 30 nM) during functionalization.[67] Using this strategy, we were able to decrease the rate difference between k_2 and k_3 by 6.84-fold (Figure S6c,d), which reduced the gain of the assay from ∼103 to ∼50% (Figure 3f). Overall, these results highlight that the gain of the signaling cascade can be optimized by simply varying the rates of k_2 and k_3, which was realized simply here by varying the concentration of aptamer or the density of the capturing DNA on the electrode. Alternatively, strategies such as modifying DNA sequences and composition,[34] using toehold-mediated strand displacement reactions,[36−39] or employing multivalent and allosteric mechanisms[14] could also be adopted to regulate the kinetics of DNA interactions.

Kinetically Controlled Signaling Cascades Are Relatively Insensitive to Thermodynamic Variations. The performance of biosensors is typically dictated by the interaction between the receptor and the target. However, typical biosensors working under thermodynamic equilibrium are also largely sensitive to various additional parameters, including the folding and interacting energies of their components. These, therefore, require specific, and tedious optimization.[9,17,68] We therefore explored whether our kinetically programmed signaling cascade required a similar level of optimization. For this purpose, we performed numerical simulations, which demonstrated the insensitivity of the kinetic assay (5 min) to variation in K_{D2} and K_{D3}. In contrast, these modifications had a huge impact on the performance of the same assay performed at equilibrium (Figure S8). To validate this experimentally, we have tested a set of signaling DNA with increasing affinity (length) for the aptamer (decreased K_{D2}) and a set of capturing DNA with an increasing affinity for the signaling DNA (decreased K_{D3}). Increasing the hybridization length is known to decrease k_{off} proportionally with the number of added Watson−Crick base pair.[69,70] On the other hand, increasing hybridization length above 7 nucleotides, typically has little impact on the k_{on},[69,70] although this remains complex to predict depending on the aptamer fold (see notes in Figure S8). Our simulation was well validated experimentally: increasing the affinity between the aptamer and signaling DNA (K_{D2}) by 5.5 kcal/mol (from 14 to 18 Watson−Crick base pairs, Table S2) did not significantly affect the gain of the cascade (between ∼70 and ∼103% at 5 min in the presence of 100 μM quinine—Figure 4a). We noticed a significantly lower gain (∼20%) only when the affinity between the aptamer and signaling DNA was reduced to the point of preventing their interaction (e.g., 12 Watson−Crick base pairs).

A similar trend was also observed when varying the K_{D3}, the affinity between the signaling and capturing DNA. For example, a variation of up to 6.0 kcal/mol in the affinity between the signaling DNA and capturing DNA (from 12 to 16 Watson−Crick base pairs, Table S3) only produced a slight gain change from ∼88 to ∼103% in the presence of 100 μM quinine (Figure 4b). Again, the gain was significantly affected only when the affinity between the signaling and capturing DNA was not enough to drive hybridization between these components (e.g., 10 Watson−Crick base pairs; ∼24% gain with less than 20 nA current after 5 min). The relative insensitivity of the signaling cascade to variation in signaling−capturing DNA affinity contrasts with the substantial effects

https://doi.org/10.1021/jacs.5c12059
J. Am. Chem. Soc. 2025, 147, 39452−39463

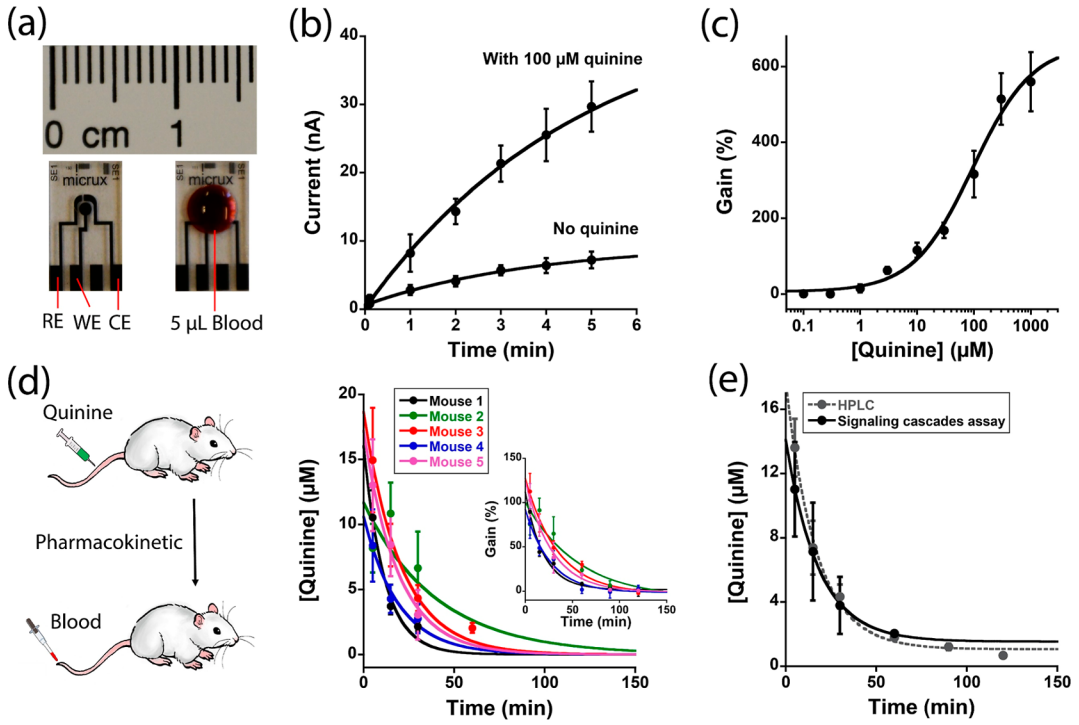

Figure 6. Therapeutic drug monitoring using an electrochemical sensor based on the kinetically programmed signaling cascade. (a) The signaling cascade assay can be performed directly in 5 μL of whole blood on a tiny integrated sensor (Micrux electrode, RE = reference electrode, WE = working electrode, and CE = counter electrode). (b) Electrochemical current kinetics when performing the assay in 5 μL of mouse blood with 100 μM or no quinine. (c) Dose–response curve of the quinine assay in mouse blood after 5 min of incubation. Of note, the quinine concentration could be measured down to about 2 μM, the detection limit of the quinine sensor in mouse blood (Figure S14). (d) We measured the pharmacokinetics of quinine (10 mg/kg of body weight) in 5 mice using the signaling cascade assay. The elimination rate constants varied from 0.025 to 0.086 min^{-1}. (e) Similar pharmacokinetics and elimination rate constants were found in 5 additional mice when employing the gold standard HPLC assays that require a 20 μL sample volume and hours of extraction/characterization procedures. The individual HPLC results are shown in Figure S15.

that such modifications typically exert on equilibrium-based mechanisms.[71] For example, mutations affecting a sensor's switching equilibrium by ~3 kcal/mol (about 200-fold switching equilibrium constant variation, K_S) can typically affect the signal change (or gain) by over 10-fold.[9] Overall, the relative insensitivity of the signaling cascade to variations in K_{D2} and K_{D3} provides a significant design benefit compared with conventional equilibrium-based biosensors (e.g., structure-switching sensors[71]) that require precise thermodynamic tuning (e.g., folding energies[72]). For example, employing a relatively long 16-nucleotides signaling DNA should provide enough binding energy to bind to any known aptamer displaying either low or high folding energy. These results, therefore, suggest that the kinetically programmed signaling cascades can be rapidly adapted for detecting other molecule–aptamer pairs without careful and time-consuming optimization of the system thermodynamics.

The Signaling Cascade Is Modular and Readily Adaptable for the Detection of Other Targets. To highlight the modularity of our signaling cascade and its simple design rules, we developed additional sensors for detecting ATP, thrombin, and platelet-derived growth factor (PDGF). For this purpose, we substituted the quinine-binding aptamer with these other aptamers and designed signaling DNA hybridizing to the 5′ DNA extremity of the aptamer and its corresponding capturing DNA (see DNA sequences in Supporting Information). Of note, other binding locations on the aptamer could have been explored and tested if target binding to the aptamer would not sufficiently inhibit the interaction with its complementary sequence. As shown in Figure 5, ATP molecules, thrombin, and PDGF were all successfully detected using a 5 min reaction time. Notably, all three additional sensors exhibited a robust "signal-on" response with similar maximum gains above 100% under the same detection conditions, concentrations of aptamer and signaling DNA, and electrode densities. In addition, the development of these sensors did not require any modification of the aptamers to either attach the redox moiety or to optimize their folding-unfolding thermodynamics.[17] Furthermore, all of them were engineered to achieve high surface probe density, improving electrode fabrication reproducibility and reducing electrode aging.[73] It is worth noting that the dynamic range and detection limit (see Figure S9) of these sensors also display a ~10 000-fold variation (e.g., the $C_{50\%}$ from 76 nM of thrombin to 0.7 mM of ATP, and the detection limit from 17 nM of thrombin to 0.15 mM of ATP), which correlates well with the variation in binding affinities of the employed aptamers (20 000-fold difference between K_D of thrombin aptamer–0.5 nM[74,75] and ATP aptamer–10 μM[76,77]). Moreover, even the slower ligand–aptamer interactions (such as the thrombin-aptamer system[78,79]) did not impact the performance nor the detection limit of the assay (see also Figure S5d,e for simulations). Overall, these results highlight the universality and simplicity of the kinetically programmed DNA-based signaling cascade design.

https://doi.org/10.1021/jacs.5c12059
J. Am. Chem. Soc. 2025, 147, 39452–39463

The Signaling Cascade Transduces Efficiently in Whole Blood and Is Multiplexable. To demonstrate the ability of our kinetically programmed signaling cascade to detect target molecules in a complex matrix, we then showed the detection of quinine directly in whole blood. We first demonstrated that blood does not interfere with the electrochemical measurements of our signaling DNA (methylene blue electrochemistry) and does not affect the performance of the signaling cascade (Figure S10). For example, we found that our electrochemical assay displayed no background in blood and provided gains similar to those obtained in buffer (90% versus 103% for 100 μM quinine detection, respectively). As expected, we also noticed that the signaling mechanism of our assay is not affected by the nonspecific adsorption of blood proteins on the sensor surface (Figure S11a). This is because the redox element is attached to the signaling DNA, and its hybridization efficiency is not significantly affected by the complex biological matrix.

Another advantage of signaling cascades is their high selectivity and specificity, which enable them to function simultaneously inside a small sample volume (e.g., inside a cell). Taking advantage of this critical feature and the barcoding ability of DNA, we tested whether the signaling cascade can be performed in a multiplexed environment together with another known hybridization-based assay[46] (Figure S11). To illustrate this, we conducted the quinine signaling cascade assay alongside another electrochemical DNA hybridization assay that detects large molecules (e.g., antibodies) via steric hindrance,[46] using the same blood sample (Figure S11b). For this purpose, we fabricated two rod electrodes, each functionalized with a specific capturing DNA (i.e., one for each assay), and these "multiplexed assays" provided similar performance when performed simultaneously in the same blood sample (Figure S11c,d). We further validated the high selectivity and specificity of DNA signaling cascades by performing NUPACK simulations[80,81] on all 12 DNA components employed in the four signaling cascades developed in this work. These simulations predict that no significant interference or crosstalk (nonspecific hybridization) would be detected even if the four signaling cascades were performed simultaneously in the same sample (Figure S12). Together, these results suggest that signaling cascades can be deployed directly in whole blood and be performed simultaneously in a multiplexed format to detect multiple targets in the same blood sample.

Adapting the Signaling Cascade into a Rapid, One-Step, Digital, Quantitative Sensor. To illustrate the usefulness of the kinetically programmed signaling cascade for health monitoring, the quinine assay was transformed into an affordable sensor that enables therapeutic drug monitoring (TDM) using just a single drop of blood. Convenient strategies enabling the monitoring of quinine and other antimalarial drugs at home would represent a significant breakthrough to improve the efficacy and effectiveness of these treatments.[60] To develop an inexpensive sensor that would require only a small blood volume, we employed Micrux electrodes (ED-SE1-AuPt) that contained three electrodes (0.08 cm diameter gold working electrode with platinum counter and reference electrodes) that only required 5 μL of sample (Figure 6a). To further optimize the gain of the quinine assay, we employed an aptamer-signaling ratio of 3:1 (Figure S13) that provided a large 316% gain after 5 min of reaction in the presence of 100 μM quinine in 5 μL of mouse blood (Figure 6b,c). Using these conditions, we characterized the dynamic range of the quinine sensor in blood (Figure 6c) and found that its optimal sensitivity aligns well with the recommended therapeutic peak plasma quinine concentration (World Health Organization recommendation: 5.27−17.9 μg/mL or 16−55 μM).[82] We subsequently performed pharmacokinetic studies in five mice administered quinine at a dose of 10 mg/kg body weight, a clinically relevant dose. The observed elimination rate constants differed by up to approximately 3-fold between individual mice (Figure 6d). Since gold standard HPLC analysis for quinine detection requires much more blood volume (20 μL for analysis) to perform simultaneous analysis on both approaches (a maximal amount of 20 μL could be collected for each time point in mice), we also performed pharmacokinetic profiling on five additional mice using HPLC measurements. These results revealed a similar average elimination rate constant and kinetics variation (3-fold) across mice samples (Figures 6e and S15). Our signaling cascade assay is achievable in a single 5 min step using only 5 μL of whole blood, while HPLC demands extensive pretreatment, prolonged analysis, and more than 20 μL of blood. This slow HPLC turnaround time, from sample collection to data assessment, typically prevents the use of TDM to optimize treatment via real-time dosage adjustments.

To illustrate how our signaling cascade could be adapted into an easy-to-use sensor capable of enabling at-home TDM, we further developed a workflow similar to that of currently commercialized lateral flow assays (Figure S16).[83] In this simple workflow architecture, the aptamer and signaling DNA are coated on the bottom and on the lid of a small Eppendorf tube, respectively. A small blood sample, 10 μL, is then conveniently added using an Aqua-Cap (Figure S16). Through a simple 10−20 s manual mixing of this Eppendorf tube, we demonstrated the detection of quinine in 10 μL of blood in 5 min. Overall, these results show that the kinetically programmed signaling cascades perform well in a one-pot format, which allows a simple one-step workflow that can be performed by untrained users.

DISCUSSION

In this study, we drew inspiration from natural cell signaling cascades to develop a simple DNA-based cascade composed of four modules and three molecular reactions, designed to detect target molecules via an electrochemical output. We first designed and validated this cascade using simulations and experiments and showed that specific kinetic tuning drastically improves its performance (rate, gain, and sensitivity). For example, the signaling cascade generated a maximum "signal-on" gain of 560% for detecting quinine directly in whole blood, compared to only 40−60% gain from the original sensor based on the same aptamer.[84,85] We also highlighted the relative insensitivity of this kinetically controlled cascade to changes in the affinity of its components. We then demonstrated the modularity and potential universality of the system by adapting it to detect four different molecular targets without requiring thermodynamic optimization. Notably, the cascade operated directly in a 5 μL drop of unprocessed blood using a simple, one-step, 5 min procedure, eliminating the need for separation, washing, or purification steps typically required by centralized laboratory methods.

Throughout the last 25 years, many research groups have pursued the development of potentially universal sensing platforms for point-of-care applications. Despite significant

https://doi.org/10.1021/jacs.5c12059
J. Am. Chem. Soc. 2025, 147, 39452−39463

progress, several technological hurdles continue to impede the translation of these systems into practical, commercial point-of-care devices (see recent reviews[68,86−88]). Key challenges include: (1) achieving reliable performance within the first few minutes of exposure to whole blood, despite biofouling; (2) designing simple, modular sensors that do not require receptor modification or complex thermodynamic tuning (e.g., optimized folding energies, precise redox element placement); and (3) implementing signaling mechanisms that avoid the need for precise surface-density optimization while still providing high signal-on gain. Our kinetically programmed signaling cascades address all of these limitations. Our approach does not require long equilibration times (>5 min) in blood to mitigate biofouling effects. Our cascades also operate more rapidly (<5 min) than recently developed signaling mechanisms employing DNAzymes[63] or mRNA/ribosomes systems.[89] Additionally, the cascades require no receptor DNA modification (e.g., redox labeling or surface attachment), preserving the receptor's native specificity and affinity. Moreover, our system functions effectively at high surface densities, which enhances electrochemical current and sensor stability.[73] Currently, our signaling cascade achieves detection limits in the low nanomolar range (e.g., 17 nM for thrombin detection, see Figure 5), which is up to 100 000 times more sensitive than traditional electrochemical enzyme-based sensors like glucometers. Notably, the sensitivity could be further improved by incorporating published signal amplification strategies. For example, nanostructure electrodes,[67,90] super sandwich strategies,[91] and other amplification strategies[92] have previously enhanced the sensitivity of hybridization-based assays by up to 1000-fold.

Over the past two decades, several signaling cascades have been engineered for diverse applications, including synthetic biology, DNA computing, drug delivery, and sensing. In this work, we have demonstrated the development of one-step kinetically programmed signaling cascades that enable rapid, high-gain, and user-friendly electrochemical sensing. We believe that such kinetically programmed cascades hold promise for broader applications across chemistry and bioengineering, particularly in areas currently constrained by complex or multistep chemical workflows. Our findings also provide insight into the potential evolutionary advantages of kinetic control in biological systems. Specifically, we show that the output of our signaling cascade is predominantly governed by kinetic parameters and is relatively insensitive to thermodynamic factors, such as mutations that alter component affinities or equilibrium states. This suggests that kinetic programming may offer a robust strategy for maintaining function under varying conditions. As computational models of biochemical signaling improve, it will be increasingly valuable to investigate how natural cascades have been kinetically optimized over evolutionary time scales and whether similar design principles have been selectively preserved to ensure rapid, reliable signal processing in living organisms.

■ ASSOCIATED CONTENT

Supporting Information

The Supporting Information is available free of charge at https://pubs.acs.org/doi/10.1021/jacs.5c12059.

Materials; methods; DNA sequences; kinetic simulations; supporting figures and tables (PDF)

■ AUTHOR INFORMATION

Corresponding Author

Alexis Vallée-Bélisle − *Laboratoire de Biosenseurs & Nanomachines, Département de Chimie, Université de Montréal, Montréal, Quebec H2V 0B3, Canada; Institut de Génie Biomédical, Département de Pharmacologie et Physiologie, Université de Montréal, Montréal, Quebec H3T 1J4, Canada; Département de Biochimie et Médecine Moléculaire, Université de Montréal, Montréal, Quebec H3T 1J4, Canada;* orcid.org/0000-0002-5009-7715; Email: a.vallee-belisle@umontreal.ca

Authors

Guichi Zhu − *Institut de Génie Biomédical, Département de Pharmacologie et Physiologie, Université de Montréal, Montréal, Quebec H3T 1J4, Canada;* orcid.org/0009-0002-4610-9522

Dominic Lauzon − *Laboratoire de Biosenseurs & Nanomachines, Département de Chimie, Université de Montréal, Montréal, Quebec H2V 0B3, Canada;* orcid.org/0000-0002-7513-3233

Carl Prévost-Tremblay − *Département de Biochimie et Médecine Moléculaire, Université de Montréal, Montréal, Quebec H3T 1J4, Canada*

Arnaud Desrosiers − *Département de Biochimie et Médecine Moléculaire, Université de Montréal, Montréal, Quebec H3T 1J4, Canada*

Bal-Ram Adhikari − *Laboratoire de Biosenseurs & Nanomachines, Département de Chimie, Université de Montréal, Montréal, Quebec H2V 0B3, Canada*

Complete contact information is available at: https://pubs.acs.org/10.1021/jacs.5c12059

Author Contributions

All authors contributed to and approved the final manuscript.

Notes

We have complied with all relevant ethical regulations at the Université de Montréal (Comité de déontologie de l'expérimentation sur les animaux, CDEA).

The authors declare the following competing financial interest(s): The work presented in this manuscript was the subject of the following patent application: Vallee-Belisle, A.; Zhu, G. Kinetically programmed systems and reactions for molecular detection. U.S. provisional application 62/680,784 filed on June 5, 2018. PCT/CA2019/050756 (Filing date 31-May-2019).

■ ACKNOWLEDGMENTS

This work was supported by a Discovery grant (RGPIN-2020-06975), an Idea to Innovation grant, and the CREATE Continuous-Flow Chemistry Program from the Natural Sciences and Engineering Research Council of Canada (NSERC). A.V.-B. is a Canada Research Chair in Bioengineering and Bionanotechnology, Tier II. G.Z. acknowledges a TransMedTech Excellence Scholarship and a PROTEO fellowship. D.L. acknowledges a Fonds de recherche du Québec-Nature et technologies Scholarship. C.P.-T. acknowledges the Natural Sciences and Engineering Research Council of Canada for a doctoral scholarship. A.D. acknowledges an NSERC Scholarship (Québec, Canada). B.R.A. acknowledges a TransMedTech Excellence Scholarship. The authors thank Manon Laprise at l'Institut de Recherche Clinique de Montreal

for performing the animal experiments (quinine injection and blood collection). The authors also thank Liliana Pedro, Dr. Nancy Schoenbrunner, Dr. Vincent De Guire, and Dr. Nagarjun Narayanaswamy for their valuable comments on the manuscript and help with the experiments, and the members of the Laboratory of Biosensors & Nanomachines (LBN).

REFERENCES

(1) Kunz, H. Emil Fischer–unequalled classicist, master of organic chemistry research, and inspired trailblazer of biological chemistry. *Angew. Chem., Int. Ed.* **2002**, *41* (23), 4439−4451.
(2) Pochan, D.; Scherman, O. Introduction: Molecular Self-Assembly. *Chem. Rev.* **2021**, *121* (22), 13699−13700.
(3) Lehn, J.-M. Perspectives in Supramolecular Chemistry-From Molecular Recognition towards Molecular Information Processing and Self-Organization. *Angew. Chem., Int. Ed.* **1990**, *29* (11), 1304−1319.
(4) Thompson, L. A.; Ellman, J. A. Synthesis and Applications of Small Molecule Libraries. *Chem. Rev.* **1996**, *96* (1), 555−600.
(5) Franzini, R. M.; Neri, D.; Scheuermann, J. DNA-encoded chemical libraries: advancing beyond conventional small-molecule libraries. *Acc. Chem. Res.* **2014**, *47* (4), 1247−1255.
(6) Chen, K.; Arnold, F. H. Engineering new catalytic activities in enzymes. *Nat. Catal.* **2020**, *3* (3), 203−213.
(7) Wang, K. Y.; Zhang, J.; Hsu, Y. C.; Lin, H.; Han, Z.; Pang, J.; Yang, Z.; Liang, R. R.; Shi, W.; Zhou, H. C. Bioinspired Framework Catalysts: From Enzyme Immobilization to Biomimetic Catalysis. *Chem. Rev.* **2023**, *123* (9), 5347−5420.
(8) Zhang, R.; Yan, X.; Fan, K. Nanozymes Inspired by Natural Enzymes. *Acc. Mater. Res.* **2021**, *2* (7), 534−547.
(9) Vallée-Bélisle, A.; Ricci, F.; Plaxco, K. W. Thermodynamic basis for the optimization of binding-induced biomolecular switches and structure-switching biosensors. *Proc. Natl. Acad. Sci. U.S.A.* **2009**, *106* (33), 13802−13807.
(10) Ricci, F.; Vallée-Bélisle, A.; Porchetta, A.; Plaxco, K. W. Rational design of allosteric inhibitors and activators using the population-shift model: in vitro validation and application to an artificial biosensor. *J. Am. Chem. Soc.* **2012**, *134* (37), 15177−15180.
(11) von Krbek, L. K. S.; Achazi, A. J.; Solleder, M.; Weber, M.; Paulus, B.; Schalley, C. A. Allosteric and Chelate Cooperativity in Divalent Crown Ether/Ammonium Complexes with Strong Binding Enhancement. *Chem.—Eur. J.* **2016**, *22* (43), 15475−15484.
(12) Ortega, G.; Chamorro-Garcia, A.; Ricci, F.; Plaxco, K. W. On the Rational Design of Cooperative Receptors. *Annu. Rev. Biophys.* **2023**, *52*, 319−337.
(13) Errington, W. J.; Bruncsics, B.; Sarkar, C. A. Mechanisms of noncanonical binding dynamics in multivalent protein-protein interactions. *Proc. Natl. Acad. Sci. U.S.A.* **2019**, *116* (51), 25659−25667.
(14) Lauzon, D.; Vallée-Bélisle, A. Programing Chemical Communication: Allostery vs Multivalent Mechanism. *J. Am. Chem. Soc.* **2023**, *145* (34), 18846−18854.
(15) Bai, Y.; Luo, Q.; Liu, J. Protein self-assembly via supramolecular strategies. *Chem. Soc. Rev.* **2016**, *45* (10), 2756−2767.
(16) Lauzon, D.; Vallée-Bélisle, A. Functional advantages of building nanosystems using multiple molecular components. *Nat. Chem.* **2023**, *15* (4), 458−467.
(17) Harroun, S. G.; Prévost-Tremblay, C.; Lauzon, D.; Desrosiers, A.; Wang, X.; Pedro, L.; Vallée-Bélisle, A. Programmable DNA switches and their applications. *Nanoscale* **2018**, *10* (10), 4607−4641.
(18) Mao, X.; Liu, M.; Li, Q.; Fan, C.; Zuo, X. DNA-Based Molecular Machines. *JACS Au* **2022**, *2* (11), 2381−2399.
(19) Kholodenko, B. N. Cell-signalling dynamics in time and space. *Nat. Rev. Mol. Cell Biol.* **2006**, *7* (3), 165−176.
(20) Lim, W. A. Designing customized cell signalling circuits. *Nat. Rev. Mol. Cell Biol.* **2010**, *11* (6), 393−403.
(21) Gordley, R. M.; Bugaj, L. J.; Lim, W. A. Modular engineering of cellular signaling proteins and networks. *Curr. Opin. Struct. Biol.* **2016**, *39*, 106−114.
(22) Nair, A.; Chauhan, P.; Saha, B.; Kubatzky, K. F. Conceptual Evolution of Cell Signaling. *Int. J. Mol. Sci.* **2019**, *20* (13), 3292.
(23) Mukherji, S.; van Oudenaarden, A. Synthetic biology: understanding biological design from synthetic circuits. *Nat. Rev. Genet.* **2009**, *10* (12), 859−871.
(24) Chatterjee, G.; Dalchau, N.; Muscat, R. A.; Phillips, A.; Seelig, G. A spatially localized architecture for fast and modular DNA computing. *Nat. Nanotechnol.* **2017**, *12* (9), 920−927.
(25) Rauch, J.; Kolch, W.; Laurent, S.; Mahmoudi, M. Big signals from small particles: regulation of cell signaling pathways by nanoparticles. *Chem. Rev.* **2013**, *113* (5), 3391−3406.
(26) Linko, V.; Ora, A.; Kostiainen, M. A. DNA Nanostructures as Smart Drug-Delivery Vehicles and Molecular Devices. *Trends Biotechnol.* **2015**, *33* (10), 586−594.
(27) Qian, L.; Winfree, E. Scaling up digital circuit computation with DNA strand displacement cascades. *Science* **2011**, *332* (6034), 1196−1201.
(28) Qian, L.; Winfree, E.; Bruck, J. Neural network computation with DNA strand displacement cascades. *Nature* **2011**, *475* (7356), 368−372.
(29) Liu, H.; Yang, Q.; Peng, R.; Kuai, H.; Lyu, Y.; Pan, X.; Liu, Q.; Tan, W. Artificial Signal Feedback Network Mimicking Cellular Adaptivity. *J. Am. Chem. Soc.* **2019**, *141* (16), 6458−6461.
(30) Yang, Q.; Guo, Z.; Liu, H.; Peng, R.; Xu, L.; Bi, C.; He, Y.; Liu, Q.; Tan, W. A Cascade Signaling Network between Artificial Cells Switching Activity of Synthetic Transmembrane Channels. *J. Am. Chem. Soc.* **2021**, *143* (1), 232−240.
(31) Han, D.; Wu, C.; You, M.; Zhang, T.; Wan, S.; Chen, T.; Qiu, L.; Zheng, Z.; Liang, H.; Tan, W. A cascade reaction network mimicking the basic functional steps of adaptive immune response. *Nat. Chem.* **2015**, *7* (10), 835−841.
(32) Wang, S.; Yue, L.; Shpilt, Z.; Cecconello, A.; Kahn, J. S.; Lehn, J. M.; Willner, I. Controlling the Catalytic Functions of DNAzymes within Constitutional Dynamic Networks of DNA Nanostructures. *J. Am. Chem. Soc.* **2017**, *139* (28), 9662−9671.
(33) Lin, N.; Ouyang, Y.; Qin, Y.; Karmi, O.; Sohn, Y. S.; Liu, S.; Nechushtai, R.; Zhang, Y.; Willner, I.; Zhou, Z. Spatially Localized Entropy-Driven Evolution of Nucleic Acid-Based Constitutional Dynamic Networks for Intracellular Imaging and Spatiotemporal Programmable Gene Therapy. *J. Am. Chem. Soc.* **2024**, *146* (30), 20685−20699.
(34) Ashwood, B.; Tokmakoff, A. Kinetics and dynamics of oligonucleotide hybridization. *Nat. Rev. Chem.* **2025**, *9* (5), 305−327.
(35) Wong, K. L.; Liu, J. Factors and methods to modulate DNA hybridization kinetics. *Biotechnol. J.* **2021**, *16* (11), No. e2000338.
(36) Seelig, G.; Soloveichik, D.; Zhang, D. Y.; Winfree, E. Enzyme-free nucleic acid logic circuits. *Science* **2006**, *314* (5805), 1585−1588.
(37) Zhang, D. Y.; Winfree, E. Control of DNA strand displacement kinetics using toehold exchange. *J. Am. Chem. Soc.* **2009**, *131* (47), 17303−17314.
(38) Yang, X.; Tang, Y.; Traynor, S. M.; Li, F. Regulation of DNA Strand Displacement Using an Allosteric DNA Toehold. *J. Am. Chem. Soc.* **2016**, *138* (42), 14076−14082.
(39) Wu, L.; Wang, G. A.; Li, F. Plug-and-Play Module for Reversible and Continuous Control of DNA Strand Displacement Kinetics. *J. Am. Chem. Soc.* **2024**, *146* (10), 6516−6521.
(40) Engvall, E.; Perlmann, P. Enzyme-linked immunosorbent assay (ELISA). Quantitative assay of immunoglobulin G. *Immunochemistry* **1971**, *8* (9), 871−874.
(41) Heid, C. A.; Stevens, J.; Livak, K. J.; Williams, P. M. Real time quantitative PCR. *Genome Res.* **1996**, *6* (10), 986−994.
(42) Gold, L.; Janjic, N.; Jarvis, T.; Schneider, D.; Walker, J. J.; Wilcox, S. K.; Zichi, D. Aptamers and the RNA world, past and present. *Cold Spring Harbor Perspect. Biol.* **2012**, *4* (3), a003582.

https://doi.org/10.1021/jacs.5c12059
J. Am. Chem. Soc. 2025, 147, 39452−39463

(43) Joshi, A.; Mayr, M. In Aptamers They Trust: The Caveats of the SOMAscan Biomarker Discovery Platform from SomaLogic. *Circulation* **2018**, *138* (22), 2482−2485.
(44) Wang, F.; Liu, X.; Willner, I. DNA switches: from principles to applications. *Angew. Chem., Int. Ed.* **2015**, *54* (4), 1098−1129.
(45) Liu, J.; Cao, Z.; Lu, Y. Functional nucleic acid sensors. *Chem. Rev.* **2009**, *109* (5), 1948−1998.
(46) Mahshid, S. S.; Camiré, S.; Ricci, F.; Vallée-Bélisle, A. A Highly Selective Electrochemical DNA-Based Sensor That Employs Steric Hindrance Effects to Detect Proteins Directly in Whole Blood. *J. Am. Chem. Soc.* **2015**, *137* (50), 15596−15599.
(47) Mahshid, S. S.; Ricci, F.; Kelley, S. O.; Vallée-Bélisle, A. Electrochemical DNA-Based Immunoassay That Employs Steric Hindrance To Detect Small Molecules Directly in Whole Blood. *ACS Sens.* **2017**, *2* (6), 718−723.
(48) Mahshid, S. S.; Mahshid, S.; Vallée-Bélisle, A.; Kelley, S. O. Peptide-Mediated Electrochemical Steric Hindrance Assay for One-Step Detection of HIV Antibodies. *Anal. Chem.* **2019**, *91* (8), 4943−4947.
(49) Fan, J.; Tang, Y.; Yang, W.; Yu, Y. Disposable multiplexed electrochemical sensors based on electro-triggered selective immobilization of probes for simultaneous detection of DNA and proteins. *J. Mater. Chem. B* **2020**, *8* (33), 7501−7510.
(50) Li, Y.; Du, H.; Wang, W.; Zhang, P.; Xu, L.; Wen, Y.; Zhang, X. A Versatile Multiple Target Detection System Based on DNA Nano-assembled Linear FRET Arrays. *Sci. Rep.* **2016**, *6*, 26879.
(51) Tsortos, A.; Grammoustianou, A.; Lymbouridou, R.; Papadakis, G.; Gizeli, E. The detection of multiple DNA targets with a single probe using a conformation-sensitive acoustic sensor. *Chem. Commun.* **2015**, *51* (57), 11504−11507.
(52) Genot, A. J.; Zhang, D. Y.; Bath, J.; Turberfield, A. J. Remote toehold: a mechanism for flexible control of DNA hybridization kinetics. *J. Am. Chem. Soc.* **2011**, *133* (7), 2177−2182.
(53) Gareau, D.; Desrosiers, A.; Vallée-Bélisle, A. Programmable Quantitative DNA Nanothermometers. *Nano Lett.* **2016**, *16* (7), 3976−3981.
(54) Zhang, D. Y.; Seelig, G. Dynamic DNA nanotechnology using strand-displacement reactions. *Nat. Chem.* **2011**, *3* (2), 103−113.
(55) Cisse, I. I.; Kim, H.; Ha, T. A rule of seven in Watson-Crick base-pairing of mismatched sequences. *Nat. Struct. Mol. Biol.* **2012**, *19* (6), 623−627.
(56) Porchetta, A.; Vallée-Bélisle, A.; Plaxco, K. W.; Ricci, F. Using distal-site mutations and allosteric inhibition to tune, extend, and narrow the useful dynamic range of aptamer-based sensors. *J. Am. Chem. Soc.* **2012**, *134* (51), 20601−20604.
(57) Xu, S.; Zhan, J.; Man, B.; Jiang, S.; Yue, W.; Gao, S.; Guo, C.; Liu, H.; Li, Z.; Wang, J.; et al. Real-time reliable determination of binding kinetics of DNA hybridization using a multi-channel graphene biosensor. *Nat. Commun.* **2017**, *8*, 14902.
(58) Achan, J.; Talisuna, A. O.; Erhart, A.; Yeka, A.; Tibenderana, J. K.; Baliraine, F. N.; Rosenthal, P. J.; D'Alessandro, U. Quinine, an old anti-malarial drug in a modern world: role in the treatment of malaria. *Malar. J.* **2011**, *10*, 144.
(59) AlKadi, H. O. Antimalarial drug toxicity: a review. *Chemotherapy* **2007**, *53* (6), 385−391.
(60) White, N. J.; Stepniewska, K.; Barnes, K.; Price, R. N.; Simpson, J. Simplified antimalarial therapeutic monitoring: using the day-7 drug level? *Trends Parasitol.* **2008**, *24* (4), 159−163.
(61) Reinstein, O.; Yoo, M.; Han, C.; Palmo, T.; Beckham, S. A.; Wilce, M. C.; Johnson, P. E. Quinine binding by the cocaine-binding aptamer. Thermodynamic and hydrodynamic analysis of high-affinity binding of an off-target ligand. *Biochemistry* **2013**, *52* (48), 8652−8662.
(62) Stojanovic, M. N.; de Prada, P.; Landry, D. W. Aptamer-based folding fluorescent sensor for cocaine. *J. Am. Chem. Soc.* **2001**, *123* (21), 4928−4931.
(63) Pandey, R.; Chang, D.; Smieja, M.; Hoare, T.; Li, Y.; Soleymani, L. Integrating programmable DNAzymes with electrical readout for rapid and culture-free bacterial detection using a handheld platform. *Nat. Chem.* **2021**, *13* (9), 895−901.
(64) Rossetti, M.; Brannetti, S.; Mocenigo, M.; Marini, B.; Ippodrino, R.; Porchetta, A. Harnessing Effective Molarity to Design an Electrochemical DNA-based Platform for Clinically Relevant Antibody Detection. *Angew. Chem., Int. Ed.* **2020**, *59* (35), 14973−14978.
(65) Vallée-Bélisle, A.; Ricci, F.; Plaxco, K. W. Engineering biosensors with extended, narrowed, or arbitrarily edited dynamic range. *J. Am. Chem. Soc.* **2012**, *134* (6), 2876−2879.
(66) Peterson, A. W.; Heaton, R. J.; Georgiadis, R. M. The effect of surface probe density on DNA hybridization. *Nucleic Acids Res.* **2001**, *29* (24), 5163−5168.
(67) Mahshid, S. S.; Vallée-Bélisle, A.; Kelley, S. O. Biomolecular Steric Hindrance Effects Are Enhanced on Nanostructured Micro-electrodes. *Anal. Chem.* **2017**, *89* (18), 9751−9757.
(68) Downs, A. M.; Plaxco, K. W. Real-Time, In Vivo Molecular Monitoring Using Electrochemical Aptamer Based Sensors: Opportunities and Challenges. *ACS Sens.* **2022**, *7* (10), 2823−2832.
(69) Stein, J. A. C.; Ianeselli, A.; Braun, D. Kinetic Microscale Thermophoresis for Simultaneous Measurement of Binding Affinity and Kinetics. *Angew. Chem., Int. Ed.* **2021**, *60* (25), 13988−13995.
(70) Tawa, K.; Yao, D.; Knoll, W. Matching base-pair number dependence of the kinetics of DNA-DNA hybridization studied by surface plasmon fluorescence spectroscopy. *Biosens. Bioelectron.* **2005**, *21* (2), 322−329.
(71) Vallée-Bélisle, A.; Plaxco, K. W. Structure-switching biosensors: inspired by Nature. *Curr. Opin. Struct. Biol.* **2010**, *20* (4), 518−526.
(72) Wu, Y.; Ranallo, S.; Del Grosso, E.; Chamoro-Garcia, A.; Ennis, H. L.; Milosavić, N.; Yang, K.; Kippin, T.; Ricci, F.; Stojanovic, M.; et al. Using Spectroscopy to Guide the Adaptation of Aptamers into Electrochemical Aptamer-Based Sensors. *Bioconjugate Chem.* **2023**, *34* (1), 124−132.
(73) Ma, T.; Martens, I.; Bizzotto, D. Thermal Stability of Thiolated DNA SAMs in Buffer: Revealing the Influence of Surface Crystallography and DNA Coverage via In Situ Combinatorial Surface Analysis. *Langmuir* **2020**, *36* (48), 14495−14506.
(74) Tasset, D. M.; Kubik, M. F.; Steiner, W. Oligonucleotide inhibitors of human thrombin that bind distinct epitopes. *J. Mol. Biol.* **1997**, *272* (5), 688−698.
(75) Centi, S.; Tombelli, S.; Minunni, M.; Mascini, M. Aptamer-based detection of plasma proteins by an electrochemical assay coupled to magnetic beads. *Anal. Chem.* **2007**, *79* (4), 1466−1473.
(76) Huizenga, D. E.; Szostak, J. W. A DNA aptamer that binds adenosine and ATP. *Biochemistry* **1995**, *34* (2), 656−665.
(77) Nutiu, R.; Li, Y. Structure-switching signaling aptamers. *J. Am. Chem. Soc.* **2003**, *125* (16), 4771−4778.
(78) Rotem, D.; Jayasinghe, L.; Salichou, M.; Bayley, H. Protein detection by nanopores equipped with aptamers. *J. Am. Chem. Soc.* **2012**, *134* (5), 2781−2787.
(79) Hasegawa, H.; Taira, K. I.; Sode, K.; Ikebukuro, K. Improvement of Aptamer Affinity by Dimerization. *Sensors* **2008**, *8* (2), 1090−1098.
(80) Zadeh, J. N.; Steenberg, C. D.; Bois, J. S.; Wolfe, B. R.; Pierce, M. B.; Khan, A. R.; Dirks, R. M.; Pierce, N. A. NUPACK: Analysis and design of nucleic acid systems. *J. Comput. Chem.* **2011**, *32* (1), 170−173.
(81) Hao, H.; Li, Y.; Yang, B.; Lou, S.; Guo, Z.; Lu, W. Simulation-Guided Rational Design of DNA Probe for Accurate Discrimination of Single-Nucleotide Variants Based on "Hill-Type" Cooperativity. *Anal. Chem.* **2023**, *95* (5), 2893−2900.
(82) *Guidelines for the Treatment of Malaria*, 3rd ed.; World Health Organization (WHO), 2015.
(83) Zhou, Y.; Wu, Y.; Ding, L.; Huang, X.; Xiong, Y. Point-of-care COVID-19 diagnostics powered by lateral flow assay. *Trends Anal. Chem.* **2021**, *145*, 116452.
(84) Baker, B. R.; Lai, R. Y.; Wood, M. S.; Doctor, E. H.; Heeger, A. J.; Plaxco, K. W. An electronic, aptamer-based small-molecule sensor

for the rapid, label-free detection of cocaine in adulterated samples and biological fluids. *J. Am. Chem. Soc.* **2006**, *128* (10), 3138−3139.
(85) Swensen, J. S.; Xiao, Y.; Ferguson, B. S.; Lubin, A. A.; Lai, R. Y.; Heeger, A. J.; Plaxco, K. W.; Soh, H. T. Continuous, real-time monitoring of cocaine in undiluted blood serum via a microfluidic, electrochemical aptamer-based sensor. *J. Am. Chem. Soc.* **2009**, *131* (12), 4262−4266.
(86) Kim, E. R.; Joe, C.; Mitchell, R. J.; Gu, M. B. Biosensors for healthcare: current and future perspectives. *Trends Biotechnol.* **2023**, *41* (3), 374−395.
(87) Trotter, M.; Borst, N.; Thewes, R.; von Stetten, F. Review: Electrochemical DNA sensing - Principles, commercial systems, and applications. *Biosens. Bioelectron.* **2020**, *154*, 112069.
(88) Kelley, S. O. COVID-19: A Crisis Creating New Opportunities for Sensing. *ACS Sens.* **2021**, *6* (4), 1407.
(89) Sadat Mousavi, P.; Smith, S. J.; Chen, J. B.; Karlikow, M.; Tinafar, A.; Robinson, C.; Liu, W.; Ma, D.; Green, A. A.; Kelley, S. O.; et al. A multiplexed, electrochemical interface for gene-circuit-based sensors. *Nat. Chem.* **2020**, *12* (1), 48−55.
(90) Soleymani, L.; Fang, Z.; Sargent, E. H.; Kelley, S. O. Programming the detection limits of biosensors through controlled nanostructuring. *Nat. Nanotechnol.* **2009**, *4* (12), 844−848.
(91) Xia, F.; White, R. J.; Zuo, X.; Patterson, A.; Xiao, Y.; Kang, D.; Gong, X.; Plaxco, K. W.; Heeger, A. J. An electrochemical supersandwich assay for sensitive and selective DNA detection in complex matrices. *J. Am. Chem. Soc.* **2010**, *132* (41), 14346−14348.
(92) Ji, H.; Yan, F.; Lei, J.; Ju, H. Ultrasensitive electrochemical detection of nucleic acids by template enhanced hybridization followed with rolling circle amplification. *Anal. Chem.* **2012**, *84* (16), 7166−7171.

https://doi.org/10.1021/jacs.5c12059
J. Am. Chem. Soc. 2025, 147, 39452−39463